

Electrochemical determination of trace sulfur containing compounds in model fuel based on silver/polyaniline-modified electrode

Siyabonga Shoba¹, Owolabi M. Bankole¹ and Adeniyi. S. Ogunlaja^{1*}

¹Department of Chemistry, Nelson Mandela University, PO Box 77000, Port Elizabeth, 6031, South Africa

Supplementary Data Section

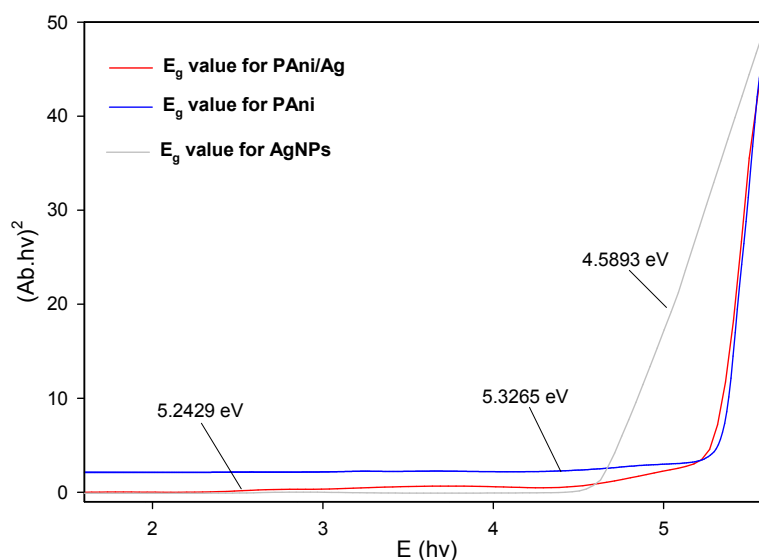
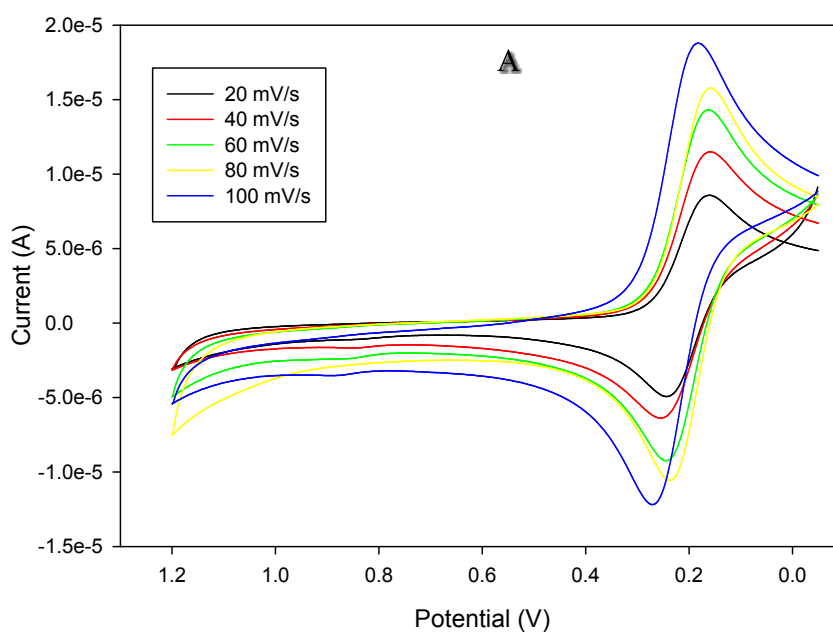


Fig. S1. Graphs showing the various energy gap (E_g)_{opt} of Ag, PANi and PANi/Ag.



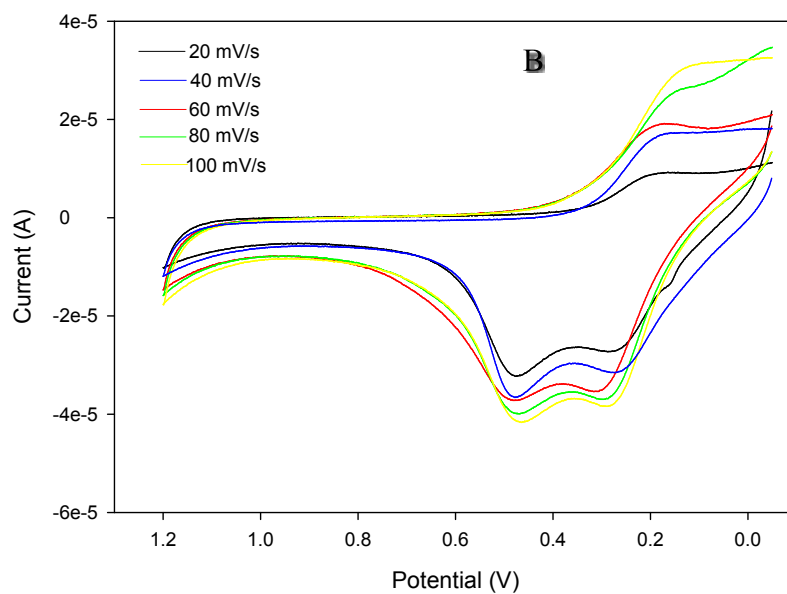


Fig S2. Graphs showing the CV at various scan rate of 20, 40, 60, 80 and 100 mV/sec using (A) GCE/PAni and (B) GCE/PAni/Ag electrode

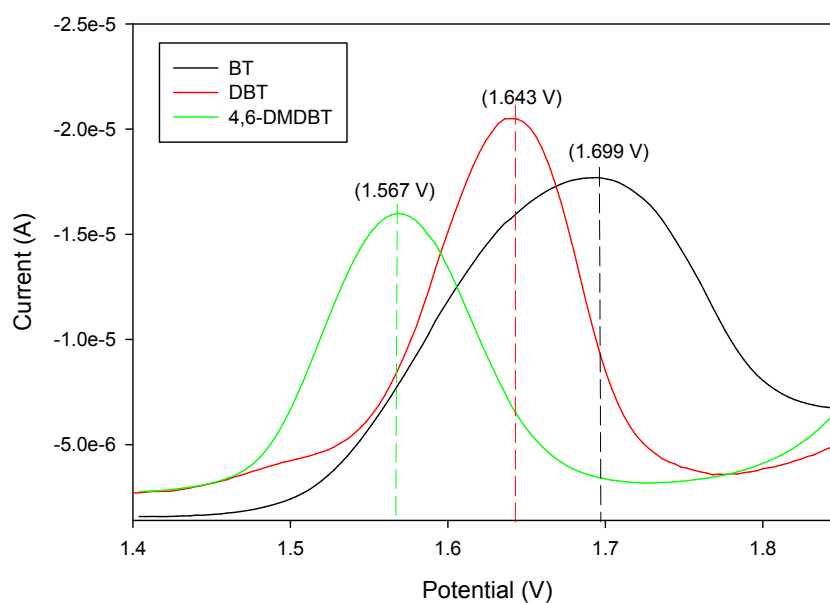


Fig. S3. Differential Pulse Voltammetry of BT, DBT and 4,6-DMDBT (10 ppm) at scan rate of 50 mV/sec showing various oxidation potentials.

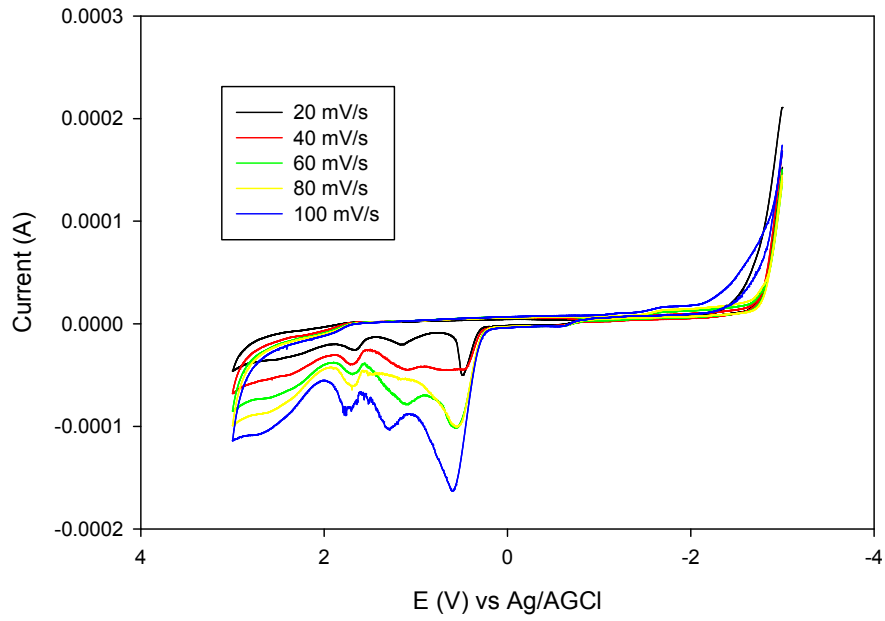


Fig. S4. Graph of peak current (mA) versus scan rate (mVs^{-1}) for 30 mg/L BT in acetonitrile.

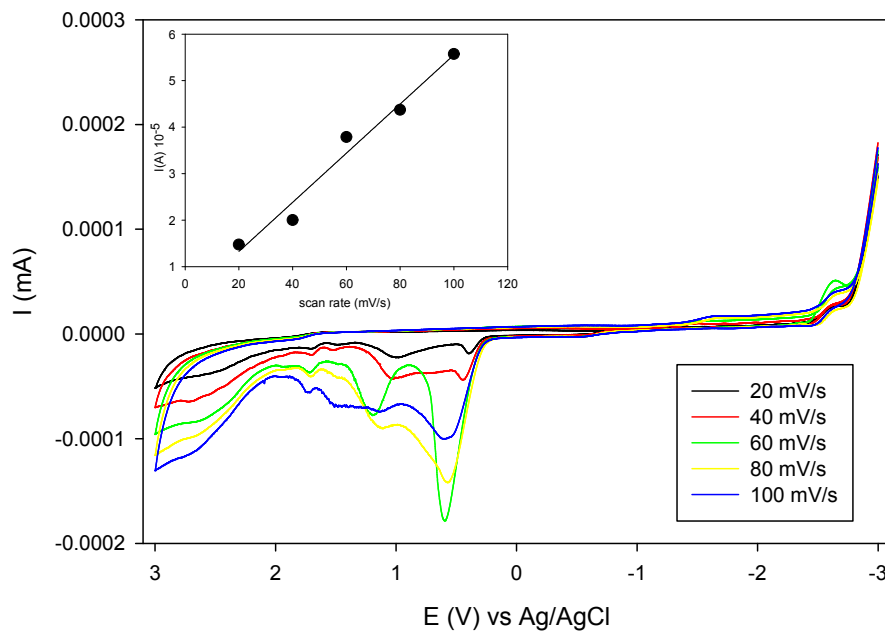


Fig. S5. Graph of peak current (mA) versus scan rate (mVs^{-1}) for 30 mg/L DBT in acetonitrile.

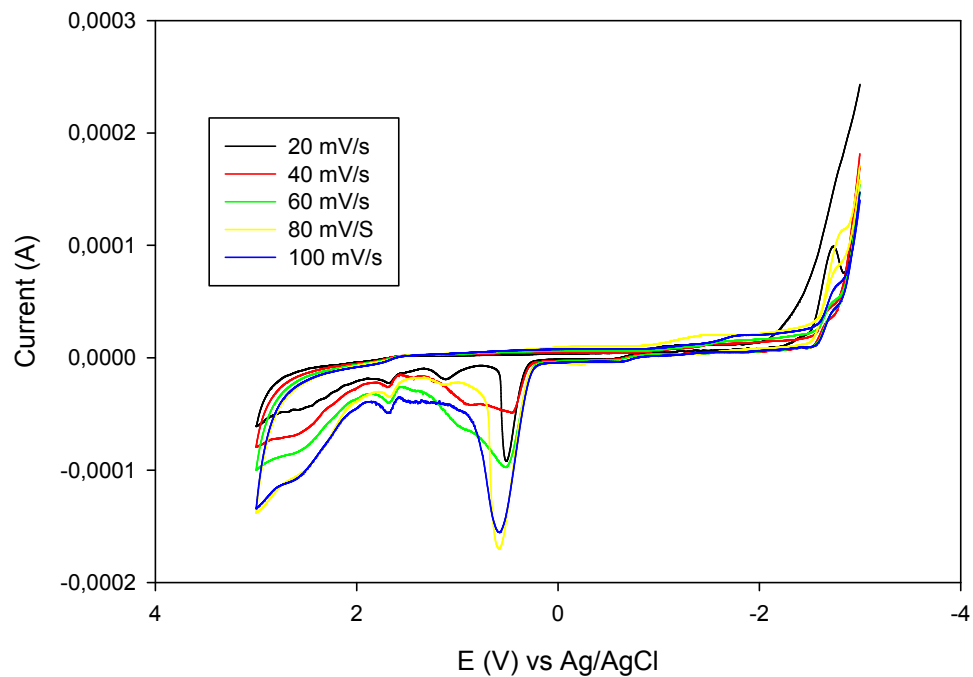


Fig. S6. Graph of peak current (mA) versus scan rate (mVs^{-1}) for 30 mg/L 4,6-DMDBT in acetonitrile.

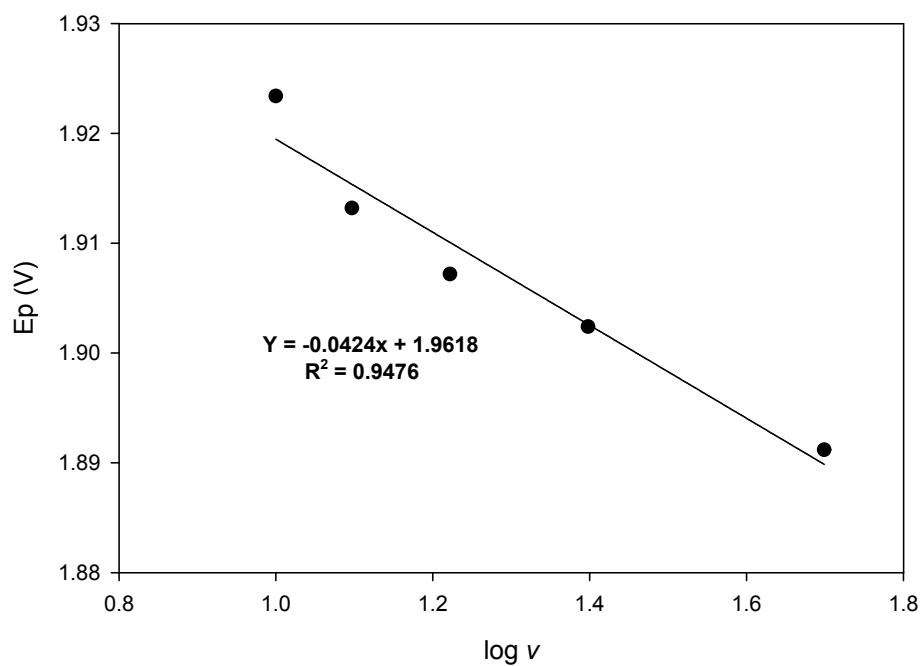


Fig. S7. Graph of E_p (V) vs. $\log v$ for BT.

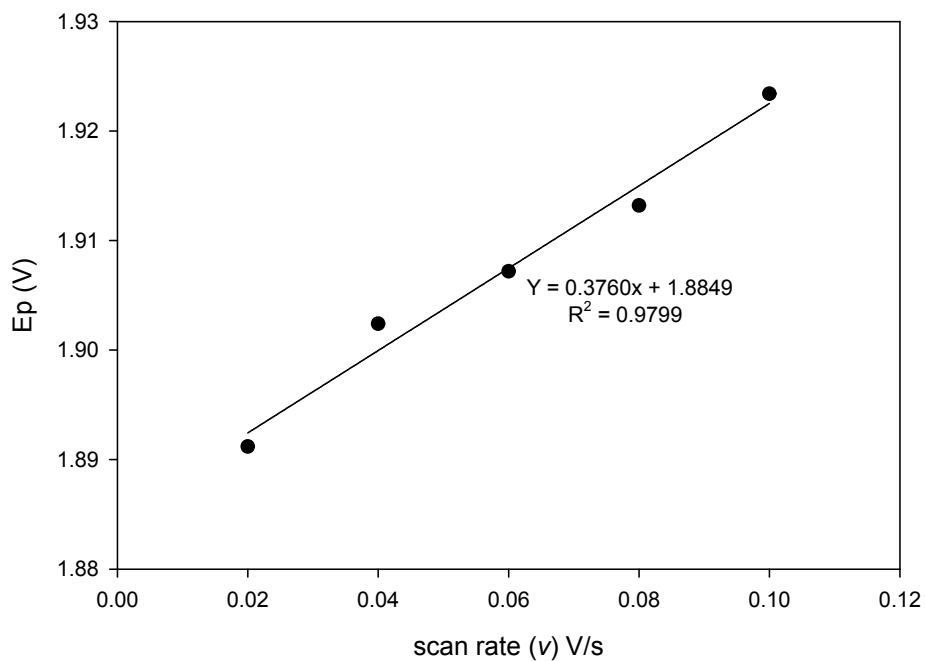


Fig. S8. Graph of E_p (V) vs. ν (V/s) for BT.

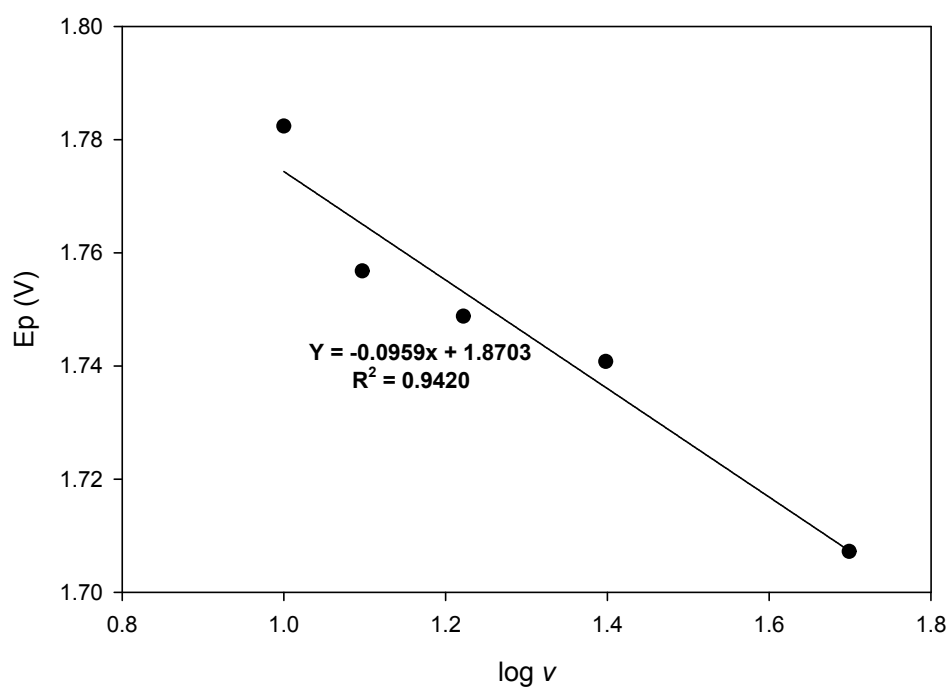


Fig. S9. Graph of E_p (V) vs. $\log \nu$ for DBT.

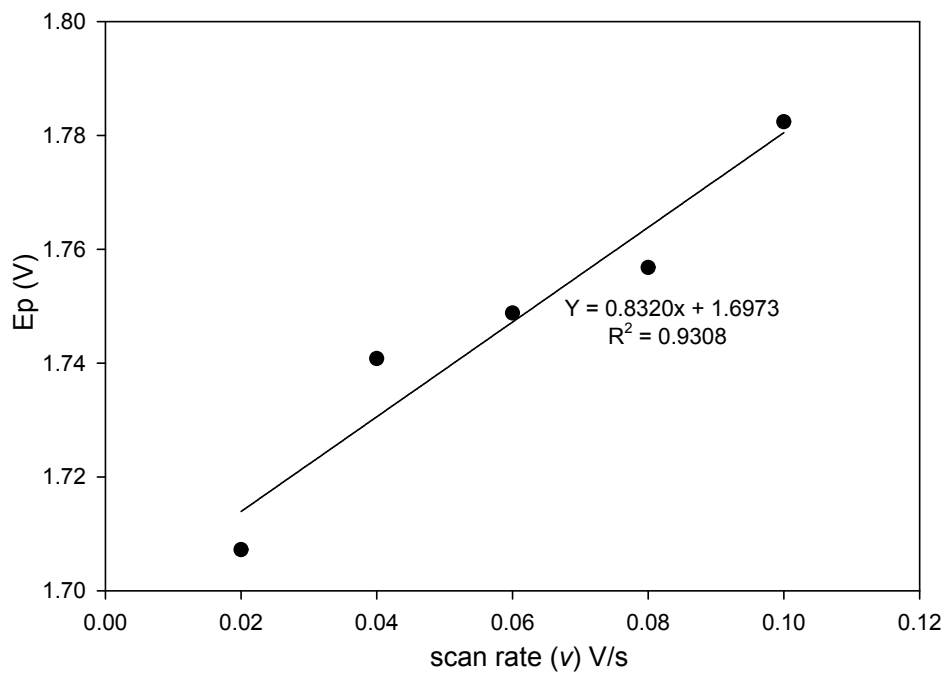


Fig. S10. Graph of E_p (V) vs. v (V/s) for DBT.

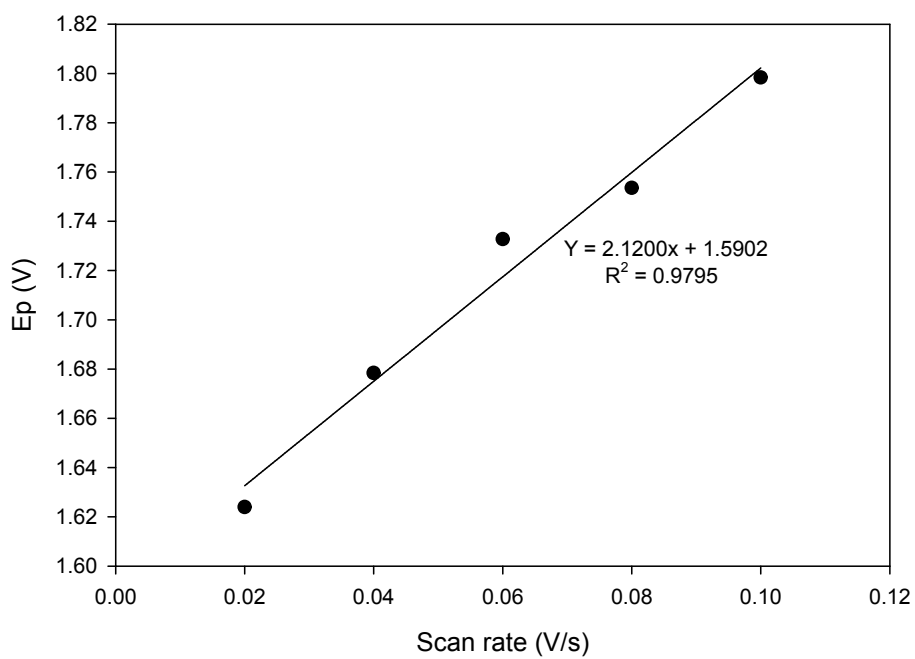


Fig. S11. Graph of E_p (V) vs. v (V/s) for 4,6-DMDBT.

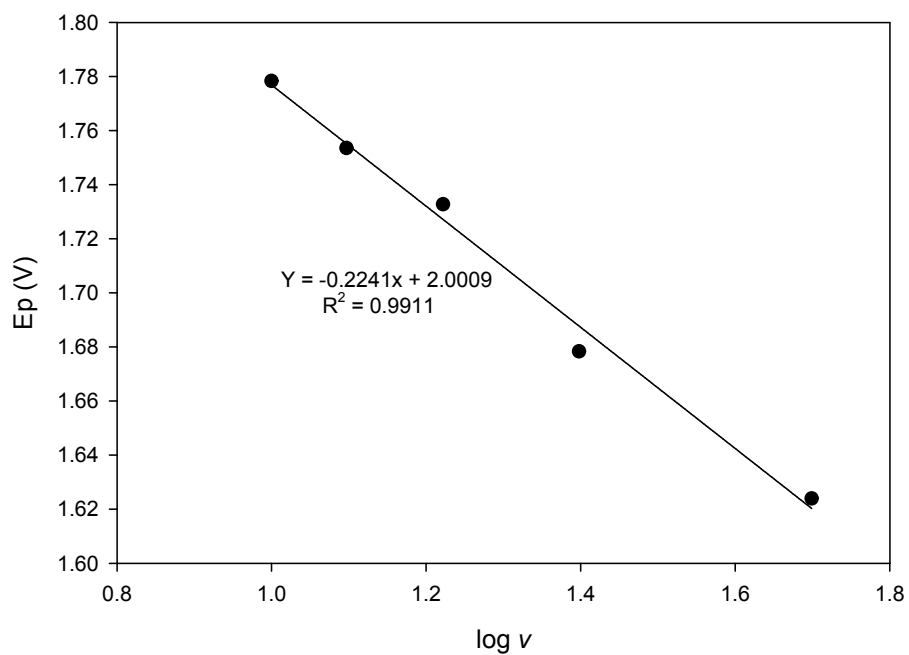


Fig. S12. Graph of E_p (V) vs. $\log v$ for 4,6-DMDBT.

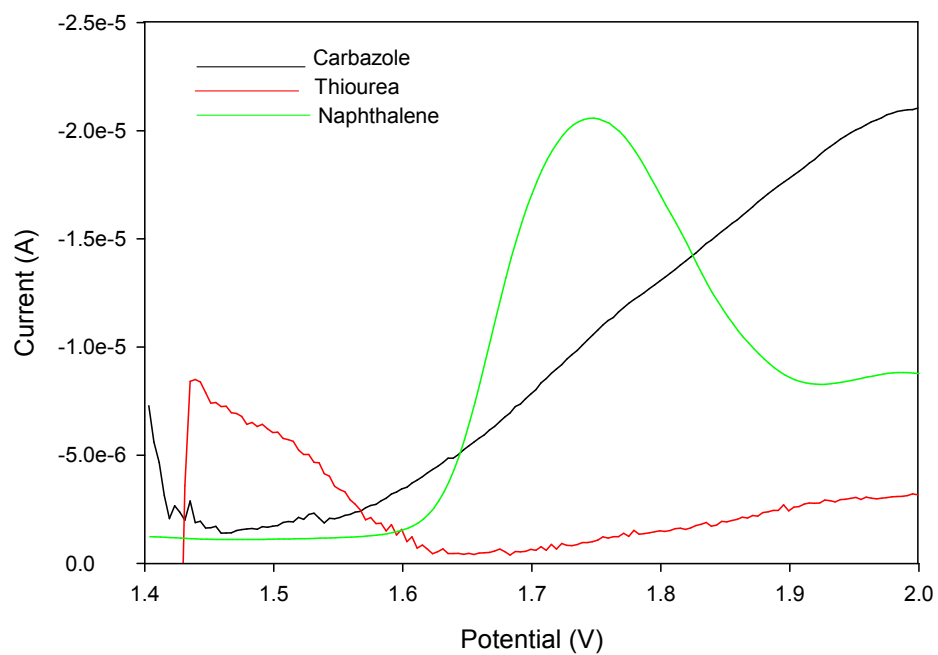


Fig. S13. DPV of carbazole, thiourea and naphthalene (100 ppm) in the range of 1.4 to 2.0 V.

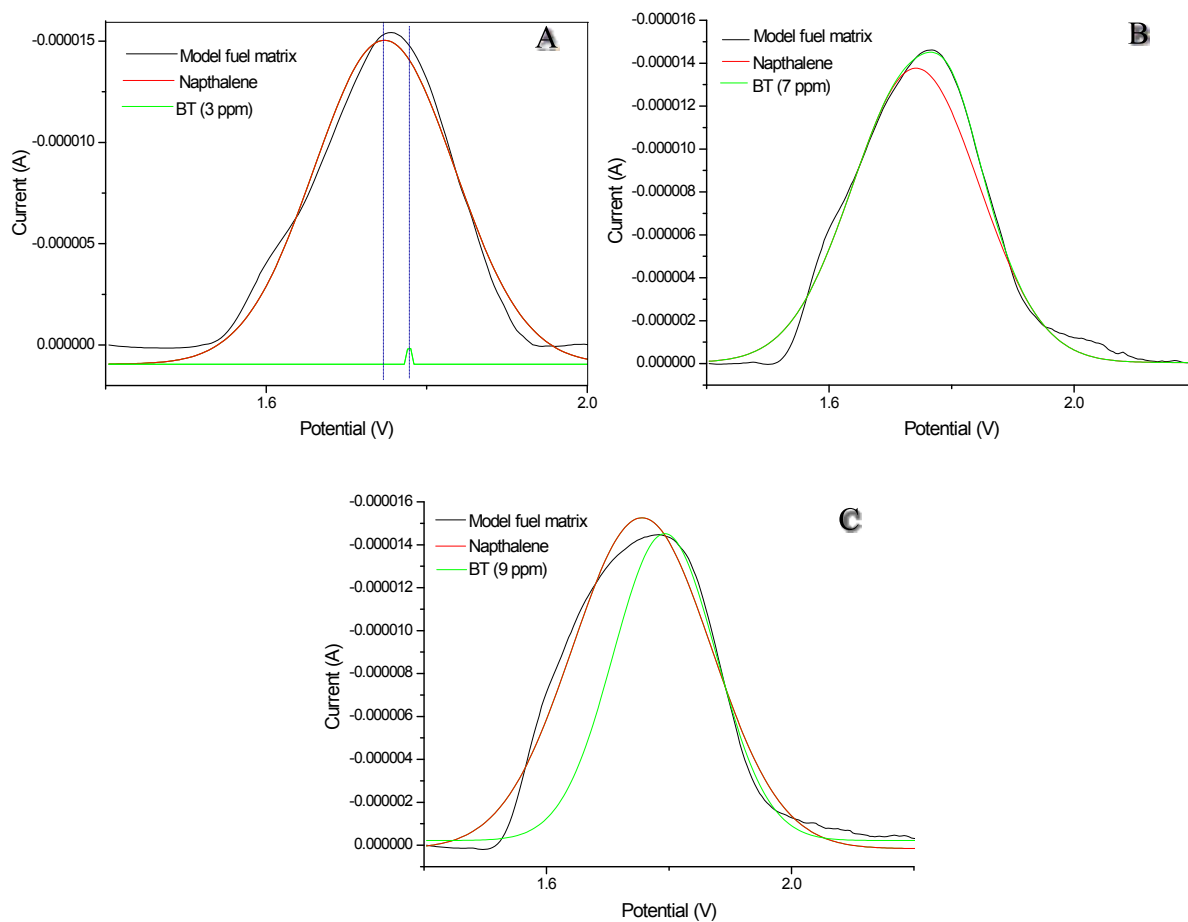


Fig. S14. DPV of model fuel (thiourea (100 ppm), carbazole (100 ppm), and naphthalene (10 ppm)) having benzothiofene concentration of (A) 3 ppm (0.72 ppmS); (B) 7 ppm (1.68 ppmS) and (C) 9 ppm (2.16 ppmS).

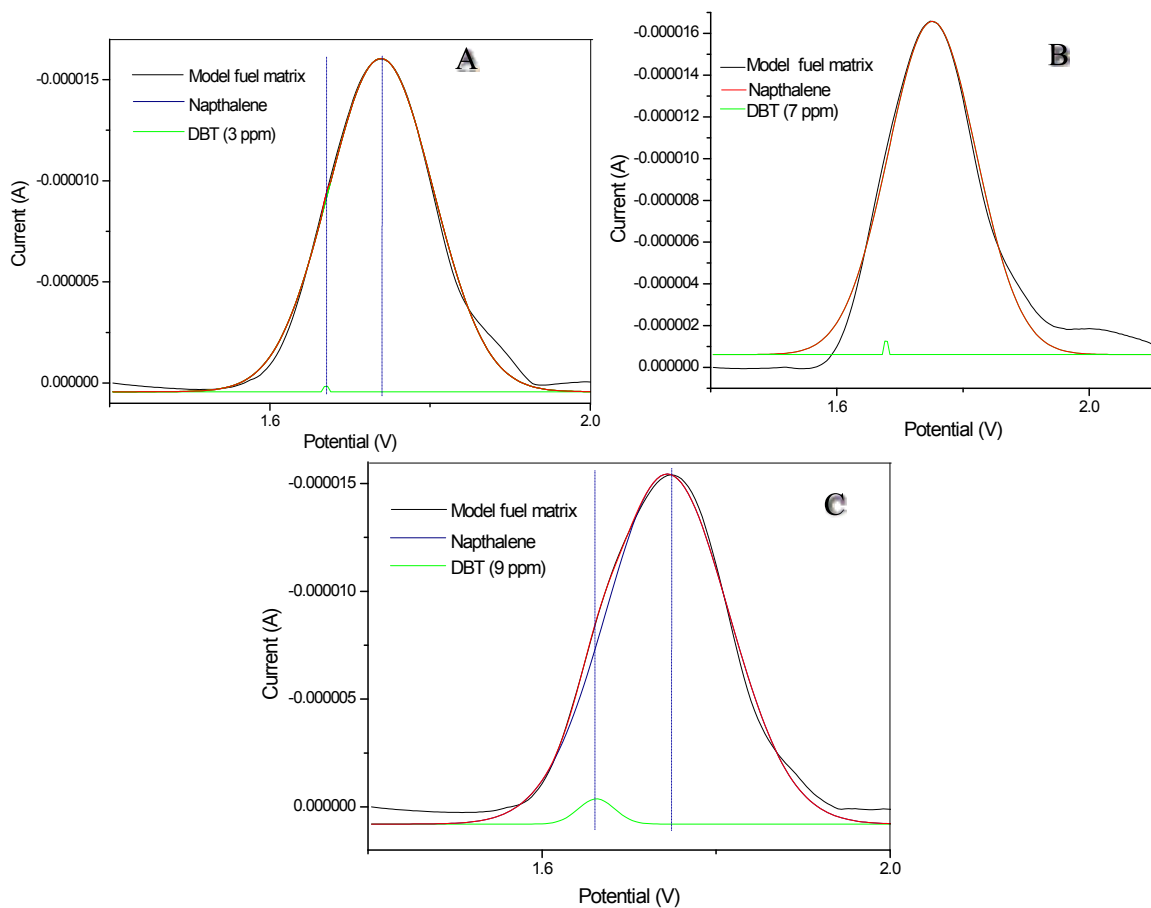
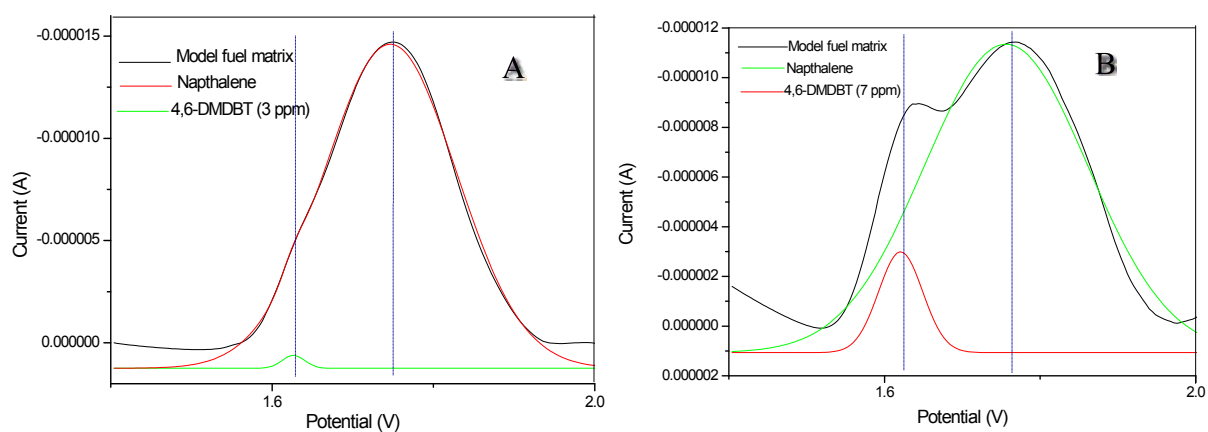


Fig. S15. DPV of model fuel (thiourea (100 ppm), carbazole (100 ppm), and naphthalene (10 ppm)) having dibenzothiophene concentration of (A) 3 ppm (0.51 ppmS); (B) 7 ppm (1.19 ppmS) and (C) 9 ppm (1.53 ppmS).



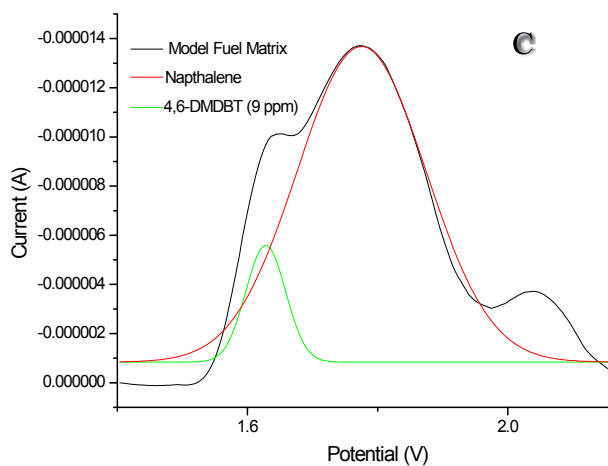


Fig. S16. DPV of model fuel thiourea (100 ppm), carbazole (100 ppm), and naphthalene (10 ppm) having 4,6-dimethyl dibenzothiophene concentration of (A) 3 ppm (0.45 ppmS), (B) 7 ppm (1.05 ppmS) and (C) 9 ppm (1.35 ppmS).

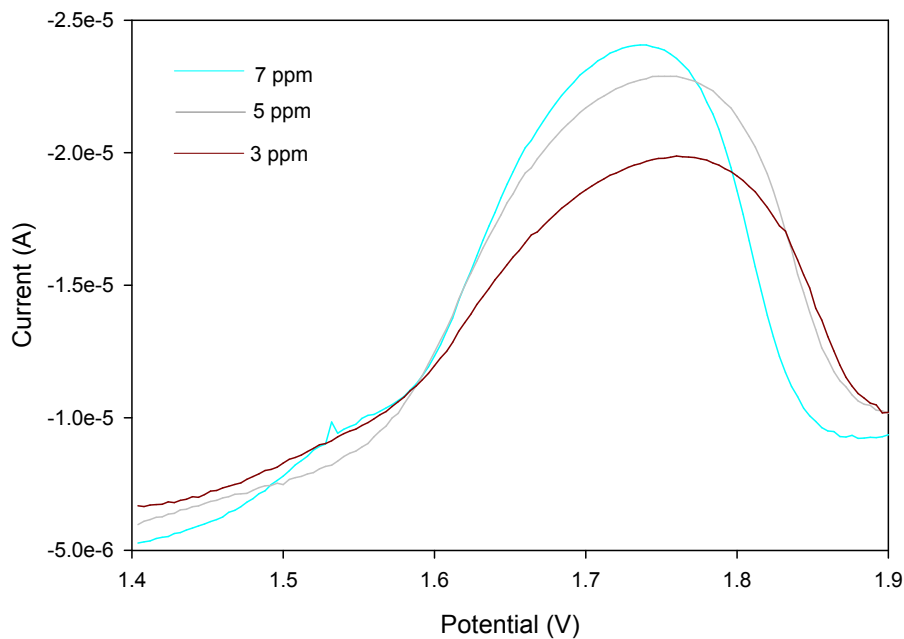


Fig. S17. DPV of various concentrations of BT (3, 5 and 7 ppm) in thiourea (100 ppm), carbazole (100 ppm), and naphthalene (10 ppm) at scan rate of 50 mV/sec.

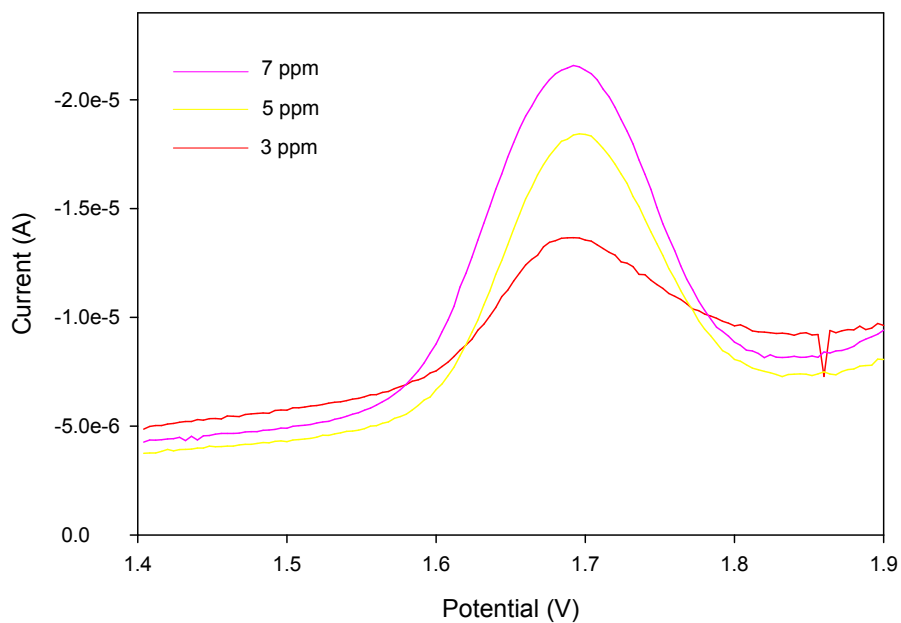


Fig. S18. DPV of various concentrations of DBT (3, 5 and 7 ppm) in thiourea (100 ppm), carbazole (100 ppm), and naphthalene (10 ppm) at scan rate of 50 mV/sec.

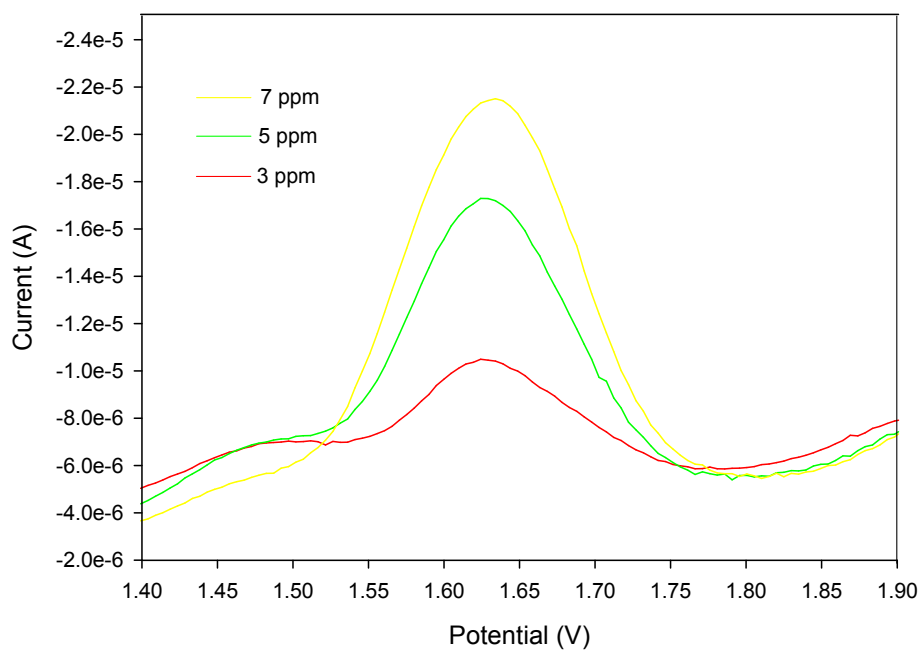


Fig. S19. DPV of various concentrations of 4,6-DMDBT (3, 5 and 7 ppm) in thiourea (100 ppm), carbazole (100 ppm), and naphthalene (10 ppm) at scan rate of 50 mV/sec.

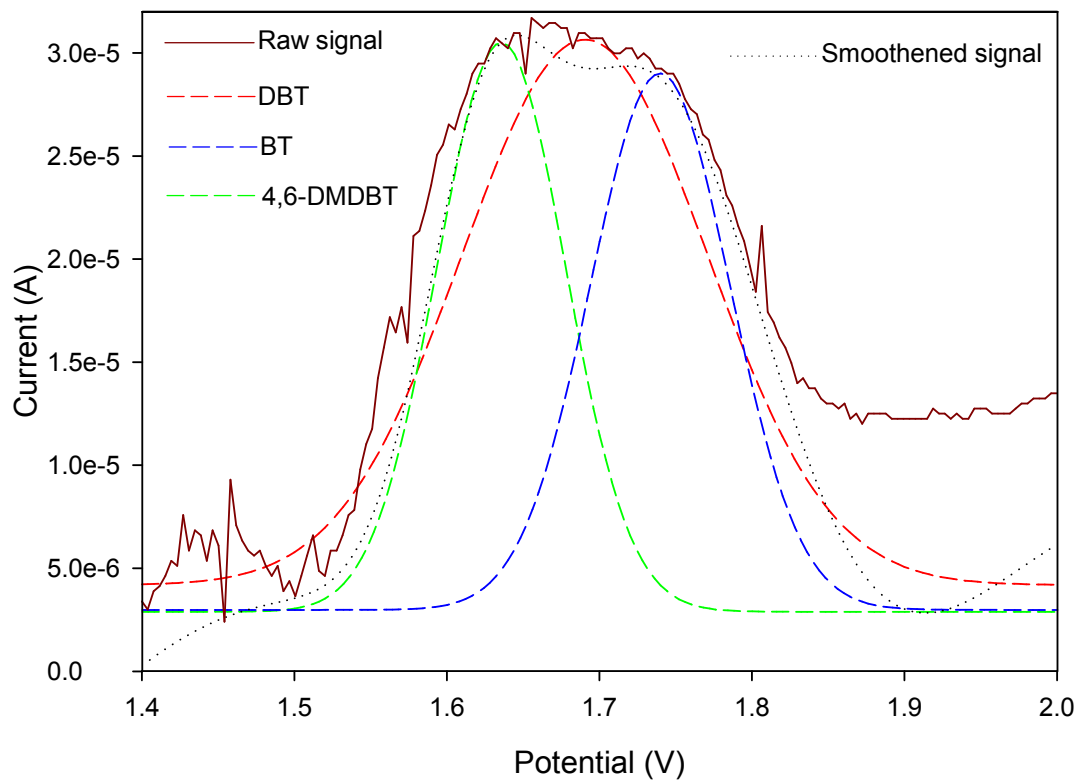


Fig. S20. Deconvoluted DPV scan showing the region where BT, DBT and 4,6-DMDBT are present in the spiked oil (10 ppm). Smoothened baseline signal was corrected prior to the deconvolution.

	BT (μA)	DBT (μA)	4,6-DMDBT (μA)
5 ppm (STANDARD)	8.5	9.0	8.9
7 ppm (STANDARD)	11.4	11.5	10.9
ULS + 5 ppm	8.1	10	7.9
ULS + 7 ppm	12	12.5	11.2
	% Recovery	% Recovery	% Recovery
% (ULS + 5 ppm)	95.3	108.7	90.5
% (ULS + 7 ppm)	104.3	107.8	101.8